

# Information entropy based algorithm of sensor placement optimization for structural damage detection

S.Q. Ye and Y.Q. Ni\*

*Department of Civil and Structural Engineering, The Hong Kong Polytechnic University,  
Hung Hom, Kowloon, Hong Kong*

*(Received February 22, 2012, Revised April 13, 2012, Accepted June 8, 2012)*

**Abstract.** The structural health monitoring (SHM) benchmark study on optimal sensor placement problem for the instrumented Canton Tower has been launched. It follows the success of the modal identification and model updating for the Canton Tower in the previous benchmark study, and focuses on the optimal placement of vibration sensors (accelerometers) in the interest of bettering the SHM system. In this paper, the sensor placement problem for the Canton Tower and the benchmark model for this study are first detailed. Then an information entropy based sensor placement method with the purpose of damage detection is proposed and applied to the benchmark problem. The procedure that will be implemented for structural damage detection using the data obtained from the optimal sensor placement strategy is introduced and the information on structural damage is specified. The information entropy based method is applied to measure the uncertainties throughout the damage detection process with the use of the obtained data. Accordingly, a multi-objective optimal problem in terms of sensor placement is formulated. The optimal solution is determined as the one that provides equally most informative data for all objectives, and thus the data obtained is most informative for structural damage detection. To validate the effectiveness of the optimally determined sensor placement, damage detection is performed on different damage scenarios of the benchmark model using the noise-free and noise-corrupted measured information, respectively. The results show that in comparison with the existing in-service sensor deployment on the structure, the optimally determined one is capable of further enhancing the capability of damage detection.

**Keywords:** structural health monitoring; sensor placement; information entropy; multi-objective optimization; damage detection; benchmark study

---

## 1. Introduction

Structural health monitoring (SHM) and damage detection is currently playing an important role in the civil engineering field. It meets the requirement to evaluate the health state of a structure immediately after undergoing natural disasters and the deterioration of a structure over its design lifespan, so that timely maintenance could be organized to avoid imminent structural failure and ensure the public safety. It is worth noting that the SHM process is directly based on the measured data obtained from the sensors mounted on the structure. However, the sensor number is usually limited, compared with the huge degrees-of-freedom (DOFs) of large-scale structures such as long-span bridges and high-rise buildings. The measured data is therefore incomplete or even insufficient.

---

\*Corresponding author, Professor, E-mail: [ceyqni@polyu.edu.hk](mailto:ceyqni@polyu.edu.hk)

A well-designed sensor configuration should make the most of the limited sensors and acquire sufficient information on structural behavior for condition assessment. Otherwise, it would restrict the ability of SHM system to successfully detect structural damage. The sensor placement problem has become an important topic in the research of SHM.

In the past two decades, considerable sensor placement optimization techniques have been developed. They can be classified mainly as three categories: (i) information-based methods, such as effective independence method (Kammer 1991), effective independence with driving point residue (Worden and Burrows 2001), and variance method (Meo and Zumpano 2005); (ii) energy-based methods, such as kinetic energy method (Heo *et al.* 1997), eigenvalue vector product method (Doebbling 1995), and non-optimal driving point method (Imamovic 1998); and (iii) information entropy based methods (Yuen *et al.* 2001, Papadimitriou 2004, 2005), which aim to study the system uncertainties and select the sensor positions that minimize the uncertainties the measured data cover. Some intelligence techniques such as genetic algorithm (Guo *et al.* 2004) and particle swarm optimization (Rao and Anadakumar 2007) have been applied to find the global optimal solutions with reduced computational efforts. Besides the above methodologies aiming at modal identification, some strategies with the purpose of damage detection (Cobb and Liebst 1996, Shi *et al.* 2000b, Souza and Epureanu 2008) have also been reported.

While sensor placement methods have been intensively studied, there are no criteria or common basis to compare the effectiveness of those sensor placement optimization techniques. In view of this awkward situation, a benchmark study on optimal sensor placement problem for the instrumented Canton Tower has been launched with intention of opening a platform for researchers to examine their own optimization strategies on the benchmark model and compare the merits and demerits of different strategies.

In this paper, the sensor placement problem for the Canton Tower and the benchmark model for this study are first detailed. Then a two-step sensor placement method for the benchmark model with the purpose of damage detection is presented. In the first step, the information that will be extracted from the monitoring data and used in a damage detection strategy is specified. In the second step, information entropy is introduced to measure the system uncertainties over the damage detection process with the use of the obtained data. Accordingly, a multi-objective optimization problem is formulated and the optimal solution is determined as the one that provides equally most informative data for all objectives. In this way, the proposed placement strategy is in line with the damage detection strategy so that the damage detection effectiveness could be maximized. To illustrate the effectiveness of the proposed sensor placement method, damage localization based on the noise-free and noise-contaminated measured mode shape change is performed respectively for detecting single- and multiple-damage incurred in the benchmark model.

## 2. Benchmark study and benchmark model

The Canton Tower (formerly named Guangzhou New TV Tower), as shown in Fig. 1, has become a landmark of Guangzhou, China since its completion of construction in 2009. It soars to 610 m in height, consisting of a main tower of 454 m high and an antennary mast of 156 m high. The structure is geometrically sophisticated with a concrete core wrapped by a triangle lattice comprising concrete-filled steel columns, rings and diagonal tubes. In synchronism with the construction progress, a long-term SHM system consisting of over 700 sensors of sixteen types has

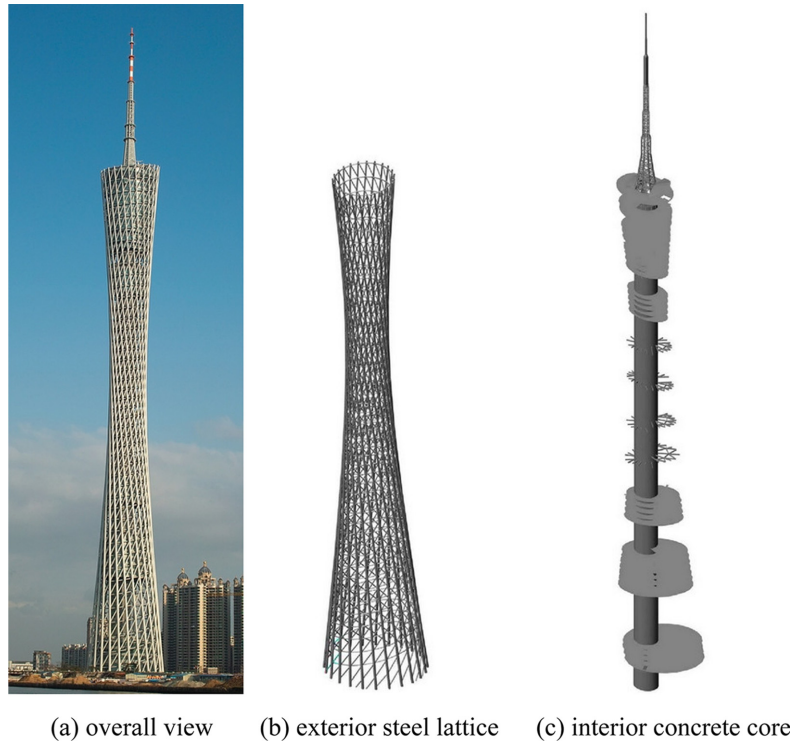


Fig. 1 The Canton Tower: (a) overall view, (b) exterior steel lattice and (c) interior concrete core

been implemented by The Hong Kong Polytechnic University on the Canton Tower to conduct real-time monitoring at both in-construction and in-service stages (Ni *et al.* 2009, 2011). Using this instrumented super-tall structure as a testbed, a series of SHM benchmark studies have been developed under the auspices of Asian-Pacific Network of Centers for Research in Smart Structure Technology (ANCRiSST). Among them, the benchmark study on sensor placement optimization focuses on determining the optimal sensor placement of accelerometers on the Canton Tower so that sufficient information about the structural behavior can be obtained for vibration-based damage detection.

An elaborate three-dimensional finite element model (FEM) of the Canton Tower has been developed with the commercial software ANSYS and validated using the identified modal properties from ambient vibration measurement. This full-scale FEM contains 122,476 elements, 84,370 nodes and 505,164 DOFs in total. However, such a model is too complex to suit it for different damage detection and sensor placement optimization algorithms. To facilitate the benchmark study, a reduced-order FEM has been reformulated which is in good agreement with the full-scale FEM in terms of both modal frequencies and mode shapes (Ni *et al.* 2012). The reduced-order FEM is a 3D cantilever beam model with 37 beam elements and 37 unconstrained nodes as illustrated in Fig. 2. Each node has 5 DOFs including 2 horizontal translations and 3 rotations. Of these, the UX and UY DOFs account for the translational displacements in the  $X$  and  $Y$  directions, while the MX, MY and MZ DOFs account for the rotations about the  $X$ -,  $Y$ - and  $Z$ -axis, respectively. In the reduced-order model, the UZ DOFs are disregarded for simplification. Thus the reduced-order model has 185 DOFs in total.

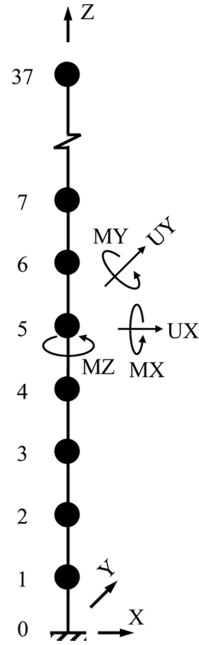


Fig. 2 A reduced-order model of the Canton Tower for benchmark study

### 3. Optimal sensor placement method

#### 3.1 Damage detection strategy

Since only the element and global mass and stiffness matrices of the reduced-order model rather than the material and geometric properties of individual structural elements are provided in the benchmark website, structural damage in an element is simulated in this study by assuming a reduction of the entire element stiffness matrix while the mass properties being kept unchanged. Thus the damage pattern is defined as

$$\Delta \mathbf{K}_k = \theta_k \cdot \mathbf{K}_k (-1 \leq \theta_k \leq 0) \quad (1)$$

where  $\mathbf{K}_k$  represents the stiffness matrix of the  $k$ th element, and  $\theta_k$  is the damage coefficient representing the percentage of the reduction in the stiffness matrix.

Thus, damage in the structure (including single- and multi-damage) can be modeled as the summation of element stiffness matrices multiplied by damage coefficients. That is

$$\Delta \mathbf{K} = \sum_{k=1}^L \theta_k \mathbf{K}_k (-1 \leq \theta_k \leq 0) \quad (2)$$

where  $L$  denotes the total number of the elements in the reduced-order model;  $\mathbf{K}_k$  and  $\theta_k$  are the  $k$ th element's stiffness matrix and its damage coefficient, respectively. The damage coefficient  $\theta_k$  is a value ranging between -1 and 0, with  $\theta_k < 0$  indicating that the element is under a damage state while with  $\theta_k = 0$  indicating that the element is not suffering from damage.

Based on the damage detection method proposed by Shi *et al.* (2000a), the change of the  $i$ th mode

shape due to the existence of damage can be represented as the summation of the contribution of each local damage to the mode shape of the structure

$$\Delta\phi_i(\theta) = \sum_{k=1}^L \theta_k \sum_{\substack{r=1 \\ r \neq i}}^N \frac{-\phi_r^T \mathbf{K}_k \phi_i}{\lambda_r - \lambda_i} \phi_r \triangleq \mathbf{F}_i(\mathbf{K})\theta \quad (3a)$$

$$\theta = \{\theta_1 \ \theta_2 \ \dots \ \theta_L\}^T \quad (3b)$$

$$\mathbf{F}_i(\mathbf{K}) = [\mathbf{F}_i(\mathbf{K}_1) \ \mathbf{F}_i(\mathbf{K}_2) \ \dots \ \mathbf{F}_i(\mathbf{K}_L)] \quad (3c)$$

$$\mathbf{F}_i(\mathbf{K}_L) \triangleq \sum_{\substack{r=1 \\ r \neq i}}^N \frac{-\phi_r^T \mathbf{K}_L \phi_i}{\lambda_r - \lambda_i} \phi_r \quad (3d)$$

where  $N$  is the number of DOFs of the structure;  $\lambda_i$  and  $\phi_i$  are the  $i$ th eigenvalue and mode shape of the undamaged structure, respectively;  $\theta$  refers to the damage coefficient vector representing the health state of each element in the structure; and  $\mathbf{F}_i(\mathbf{K})$  is defined as the sensitivity matrix of the change of the  $i$ th mode shape with respect to the damage coefficient vector  $\theta$ .

### 3.2 Optimal sensor placement

Once mode shapes before and after damage in the structure are observed, an optimal estimate for the damage coefficient vector  $\hat{\theta}$  can be inferred using the prediction model defined in Eq. (3). However, it is worth noting that there are always prediction errors between the observations and the predictions. These mismatches arise from various sources such as incomplete measured data due to limited sensor number, measurement noise, modeling error, and insufficient bandwidth of excitation and response (Beck and Katafygiotis 1998). The prediction errors will cause uncertainties in the damage detection process, resulting in uncertain level of accuracy of the solution. In particular, these uncertainties are inevitably associated with the identification process through the structural information obtained from the sensing network. In view of this, sensor layout should be designed in such a fashion that the limited measured information is more robust to the uncertainties and therefore the measured data is most informative for damage detection. Since information entropy is a direct measure of the uncertainties (Papadimitriou 2004), the sensor placement should be designed in terms of the information entropy. Let  $\mathbf{n} \in \mathbf{R}^{N_d}$  be the prediction error, the measured change of the  $i$ th mode shape of the structure satisfies the equation

$$\Delta\varphi_i(m) = \mathbf{L}_0(\delta)\Delta\phi_i(m) + \mathbf{L}_0(\delta)\mathbf{n} \quad (4)$$

where  $\Delta\varphi_i(m) \in \mathbf{R}^{N_0}$  is the sample series of the  $i$ th measured mode shape change, and  $\Delta\phi_i(m) \in \mathbf{R}^{N_d}$  is the prediction described in Eq. (3);  $N_0$  and  $N_d$  are the number of measured DOFs and the number of measurable DOFs, respectively;  $\mathbf{L}_0(\delta) \in \mathbf{R}^{N_0 \times N_d}$  is the observation matrix composed of zeros and ones, and maps the measured DOFs to the measurable DOFs; and  $\delta \in \mathbf{R}^{N_d}$  is the sensor configuration vector specifying the  $N_0$  measured DOFs with  $\delta_j = 1$  at the observed DOF and  $\delta_j = 0$  at the unobserved DOF; Particularly,  $\mathbf{L}_0^T \mathbf{L}_0 = \text{diag}(\delta)$ . According to the information entropy method proposed by Papadimitriou (2004), the uncertainties over the damage detection process can be quantified by an information entropy measure which is defined as

$$H(\mathbf{D}) = - \int p(\boldsymbol{\theta}|\mathbf{D}) \ln p(\boldsymbol{\theta}|\mathbf{D}) d\boldsymbol{\theta} \quad (5)$$

where  $\mathbf{D}$  is the measured data;  $p(\boldsymbol{\theta}|\mathbf{D})$  is the probability model specifying the probability of each possible value of  $\boldsymbol{\theta}$  based on the measured data  $\mathbf{D}$ , and can be established in terms of the optimal value  $\hat{\boldsymbol{\theta}}$  of damage coefficients and the optimal prediction error  $\hat{\sigma}$  expected for a set of test data. As shown in Eq. (5), the information entropy measure depends only on the measured data  $\mathbf{D}$  and the corresponding sensor configuration  $\boldsymbol{\delta}$ .

Since observations are not available in the sensor placement design stage, the probability model is assumed by taking the optimal values  $\hat{\boldsymbol{\theta}}$  and  $\hat{\sigma}$  as expected nominal values  $\boldsymbol{\theta}_0$  and  $\sigma_0$ . The information entropy in Eq. (5) can be asymptotically approximated by (Papadimitriou 2004)

$$H(\mathbf{D}) \sim H(\boldsymbol{\delta}, \boldsymbol{\theta}_0, \sigma_0) = \frac{1}{2} N_\theta [\ln(2\pi) + \ln \sigma_0^2] - \frac{1}{2} \ln[\det \mathbf{Q}(\boldsymbol{\delta}, \boldsymbol{\theta}_0)] \quad (6)$$

where  $N_\theta$  is the number of damage coefficients for identification; the nominal damage coefficient vector  $\boldsymbol{\theta}_0$  specifying the changes in stiffness properties of the structure can be set as the one that indicates the future damage expected for the structure; and the nominal value  $\sigma_0$  of the prediction error is chosen to be representative of the estimate system. The matrix  $\mathbf{Q}(\boldsymbol{\delta}, \boldsymbol{\theta}_0)$  appearing in Eq. (6) is a positive definite matrix and expressed as

$$\mathbf{Q}(\boldsymbol{\delta}, \boldsymbol{\theta}_0) = \sum_{j=1}^{N_d} \delta_j \mathbf{P}^{(j)}(\boldsymbol{\theta}_0) \quad (7)$$

which is known as the Fisher information matrix. It contains the information about the parameters  $\boldsymbol{\theta}$  based on the observations obtained from sensor layout  $\boldsymbol{\delta}$ . The matrix  $\mathbf{P}^{(j)}(\boldsymbol{\theta})$  is a positive semi-definite matrix of the form

$$\mathbf{P}^{(j)}(\boldsymbol{\theta}_0) = \nabla_\theta [\Delta \boldsymbol{\phi}_{ij}(\boldsymbol{\theta}_0)] \nabla_\theta^T [\Delta \boldsymbol{\phi}_{ij}(\boldsymbol{\theta}_0)] \quad (8)$$

where  $\Delta \boldsymbol{\phi}_{ij}$  denotes the  $i$ th mode shape change of the  $j$ th element of the structure in terms of the damage coefficients  $\boldsymbol{\theta}$ ; and  $\nabla_\theta = [\partial/\partial \theta_1, \dots, \partial/\partial \theta_{N_\theta}]^T$  is the gradient vector with respect to  $\boldsymbol{\theta}$ . The matrix  $\mathbf{P}^{(j)}(\boldsymbol{\theta})$  represents the contribution of each DOF measurement to the change of modal behavior regarding the damage. Substituting  $\Delta \boldsymbol{\phi}_{ij}$  given in Eq. (3) into Eq. (8), it can be further obtained as

$$\mathbf{P}^{(j)} = [\mathbf{F}_i^{(j)}(\mathbf{K}_s) \mathbf{F}_i^{(j)}(\mathbf{K}_t)]_{N_\theta \times N_\theta} \quad (9)$$

where  $\mathbf{F}_i^{(j)}(\mathbf{K}_s)$  is the  $j$ th element in the vector  $\mathbf{F}_i(\mathbf{K}_s)$ , defined as the sensitivity of the mode shape change at the  $j$ th DOF to the local damage in the  $s$ th element. As can be seen in Eq. (9), the matrix  $\mathbf{P}^{(j)}(\boldsymbol{\theta}_0)$  is independent of the nominal values  $\boldsymbol{\theta}_0$  since  $\boldsymbol{\theta}$  is eliminated through the gradient vector  $\nabla_\theta$ . It depends only on the sensitivity of the structural modal properties at the  $j$ th DOF with respect to the damage coefficients. The Fisher information matrix  $\mathbf{Q}(\boldsymbol{\delta}, \boldsymbol{\theta}_0)$  in Eq. (7) subsequently represents the sensibility towards  $\boldsymbol{\theta}$  for a specified sensor network  $\boldsymbol{\delta}$ .

In this way, the information entropy becomes a direct measure of uncertainties over the estimation process using the  $i$ th measured mode shape change, which is only associated with the sensor configuration  $\boldsymbol{\delta}$  and the designed prediction error  $\sigma_0$ . It provides a rational criterion for comparing the quality of the measured information involving different sensor configurations. If only one mode is involved in the damage detection process, the optimal sensor layout should be selected as the one that minimizes the information entropy measure among all possible configurations. That is

$$\delta_{opt} = \arg \min_{\delta} H(\delta, \sigma_0) \quad (10)$$

If several observed modes are taken into account for damage detection, the sensor placement strategy in terms of information entropy can be formulated as a multi-objective optimization problem. For convenience, the information entropy index for the  $i$ th measured mode is constructed as

$$IEI_i(\delta) = \frac{H_{i,\delta} - H_{i,\min}}{H_{i,\max} - H_{i,\min}} \quad (11)$$

where  $H_{i,\max}$  and  $H_{i,\min}$  are two reference configurations for  $N_0$  sensors, with  $H_{i,\min}$  computed for the optimal sensor configuration that results in the minimum information entropy, while with  $H_{i,\max}$  corresponding to the worst sensor configuration that yields the maximum information entropy. Let  $J_i = IEI_i(\delta)$ , the multi-objective optimization problem consisting of  $i$  objectives can be formulated as

$$\mathbf{J}(\delta) = (J_1(\delta), J_2(\delta), \dots, J_i(\delta)) \quad (12)$$

The optimal sensor placement is the one that minimizes  $\mathbf{J}(\delta)$ . For this kind of multi-objective optimal problem, instead of single optimal solution, there are a set of conflicting ones, which are optimal in a sense that they cannot be improved in any objective without compromising at least one other objective. These alternative solutions are known as Pareto optimal solutions (Srinivas and Deb 1994, Fonseca and Flemming 1995).

To find the Pareto optimal solutions, a computationally efficient technique termed forward sequential sensor placement (FSSP) proposed by Papadimitriou (2005) is applied. The Pareto optimal solutions for one sensor are first determined by an exhaustive search approach. Following this approach, all possible configurations are obtained by placing one sensor on a measurable DOF. Comparing  $\mathbf{J}(\delta)$  for each configuration and deleting those placements  $\mathbf{b}$  that satisfy

$$J_{n_i}(\mathbf{a}) \leq J_{n_i}(\mathbf{b}) \text{ for all } n_i \in \{1, 2, \dots, i\} \quad (13)$$

yield the Pareto optimal solutions for one sensor. Then the Pareto optimal configurations for  $(s+1)$  sensors are obtained iteratively from the Pareto optimal configurations for  $s$  sensors as follows. Let  $P_s^{n_s}$  be the set of all the Pareto solutions for  $s$  sensors where  $n_s$  is the solution number. For each solution  $P_s^{(i)}$ , a new set of all possible sensor configurations involving  $(s+1)$  sensors are constructed by adding one more sensor at each measurable DOF. Then, the Pareto solutions  $P_{s+1}^{n_{s+1}}$  are obtained by deleting those sensor placements  $\mathbf{b}$  that satisfy Eq. (13). This process is repeated for all Pareto configurations in  $P_s^{n_s}$ , generating a new set of Pareto solutions for  $(s+1)$  sensors. And this iteration process is continued for up to  $N_0$  sensors required. Among all the Pareto configurations, the optimal solution is selected as the one that has the minimum  $J_0$ .

#### 4. Case study

The existing in-service sensor placement for the Canton Tower includes 20 accelerometers deployed on eight sections as shown in Fig. 3. Of these, two critical sections, i.e., the waist level and the rooftop of the main tower, are each installed with four accelerometers to monitor the UX and UY DOFs, while the other six sections are each installed with two accelerometers to monitor

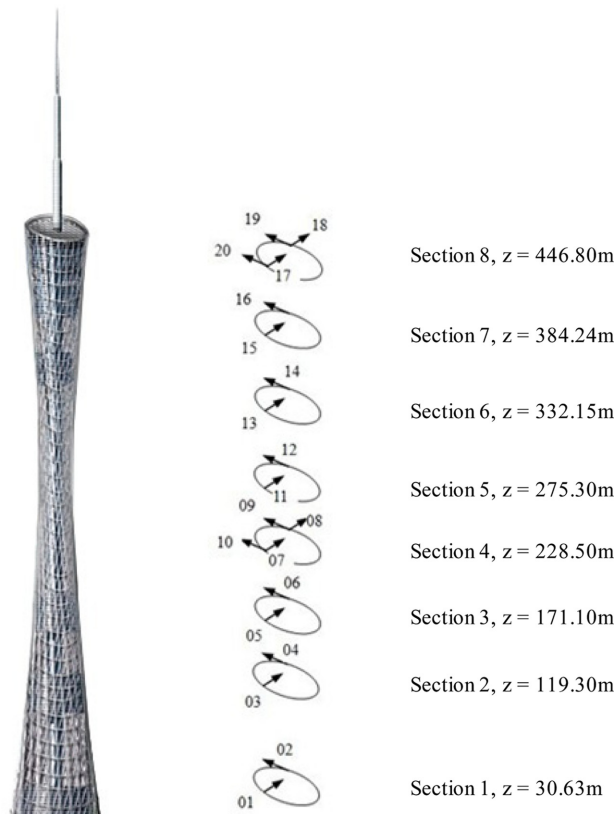


Fig. 3 The existing in-service sensor configuration for 20 accelerometers

Table 1 The existing in-service sensor placement for accelerometers on the benchmark model

| Node number | Measurement direction | Node number | Measurement direction |
|-------------|-----------------------|-------------|-----------------------|
| 4           | $X$ -axis             | 15          | $X$ -axis             |
| 4           | $Y$ -axis             | 15          | $Y$ -axis             |
| 9           | $X$ -axis             | 17          | $X$ -axis             |
| 9           | $Y$ -axis             | 17          | $Y$ -axis             |
| 12          | $X$ -axis             | 21          | $X$ -axis             |
| 12          | $Y$ -axis             | 21          | $Y$ -axis             |
| 14          | $X$ -axis             | 27          | $X$ -axis             |
| 14          | $Y$ -axis             | 27          | $Y$ -axis             |

the translational displacements in the  $X$ - and  $Y$ -directions, respectively. An equivalent 16-sensor configuration on the reduced-order model is shown in Table 1. In order to compare the existing in-service sensor placement and the optimized sensor configuration, 16 accelerometers are first involved to perform sensor placement optimization for the benchmark model. Then another optimal sensor configuration associated with 20 accelerometers (same as the number of sensors really deployed on the structure) is explored.

The proposed sensor placement method is performed on the reduced-order model with a total of

37 elements and 185 DOFs. The data obtained from the optimally determined sensor configuration will be used in damage detection. The results will be compared with those obtained from the existing in-service sensor configuration.

#### 4.1 Optimal sensor placement for 16 accelerometers

##### 4.1.1 Simulation results

Given the number of accelerometers, they should be placed judiciously so as to catch the largest amount of structural condition information. In this case study, it is assumed that the total number of accelerometers available is 16 and two translational DOFs of each node in the reduced-order model (a total of 74 translational DOFs for 37 unconstrained nodes in the model) are observable. The structure is parameterized in terms of 37 damage coefficients,  $\theta$ , with the  $i$ th coefficient indicating the change of the stiffness property in the  $i$ th member of the structure. The modal parameters at all DOFs are obtained through modal analysis on the structure, and the mode shape change in terms of damage coefficients  $\theta$  is subsequently extracted according to Eq. (3). Then the information entropy index defined in Eq. (11) is applied to construct the multi-objective function in Eq. (12) to measure the uncertainties over the estimation of  $\theta$  using the measured change of mode shapes. With the constructed multi-objective function, the FSSP algorithm is applied to estimate the optimal locations for 16 sensors on the structure. In calculating the information entropy index for the  $i$ th mode according to Eq. (11),  $H_{i,\max}$  is determined for the 1-sensor configuration that results in the minimum information entropy value for the  $i$ th mode involved, while  $H_{i,\min}$  corresponds to the sensor configuration of involving sensors at all measurable DOFs which yields the minimum information entropy value for the  $i$ th mode. The first 15 modes are considered in this case study for determining the optimal sensor placement. Table 2 provides the optimally determined sensor placement for 16 accelerometers by the proposed sensor placement optimization strategy.

It is observed that in comparison with the existing in-service sensor positions which are relatively uniformly placed on the structure, the optimized configuration is in a more compact fashion where the sensors are mainly located around the base of the structure and at the sections around the waist level which is the minimum cross sectional area of the main tower of the Canton Tower. In addition, none of the DOFs on the antenna mast is included in the configuration. It may be attributed to the fact that the antenna mast dominated modes are high-order ones with low modal participation factors (the mass of the antenna mast is much less than that of the main tower). Likewise, the sensitivity of modal shape change due to local damage at the antenna mast is considerably low for

Table 2 The optimally determined sensor placement when using 16 accelerometers

| Node number | Measurement direction | Node number | Measurement direction |
|-------------|-----------------------|-------------|-----------------------|
| 1           | X-axis                | 10          | X-axis                |
| 1           | Y-axis                | 10          | Y-axis                |
| 2           | X-axis                | 13          | X-axis                |
| 2           | Y-axis                | 13          | Y-axis                |
| 3           | X-axis                | 14          | X-axis                |
| 3           | Y-axis                | 14          | Y-axis                |
| 4           | X-axis                | 15          | X-axis                |
| 4           | Y-axis                | 15          | Y-axis                |

the main tower dominated modes accounted for in the sensor placement optimization.

#### 4.1.2 Verification

The change in pre- and post-damage mode shapes obtained from the placed sensors contains information about the damage incurred in the structure, and can be utilized for structural damage detection. In order to compare the performance of the optimally determined and the existing in-service sensor configurations in assessing structural damage, damage detection using the measured mode shapes without noise and with white noise of 5% noise-to-signal ratio is performed on four damage cases of the benchmark structure, respectively. The damage cases for the benchmark model are single damage in the 12th element, single damage in the 21st element, multi-damage in the 3rd and 35th elements, and multi-damage in the 18th and 20th elements. The damage in a specified element is assumed as a 10% reduction of the corresponding element stiffness matrix.

A simple damage indicator, multiple damage location assurance criterion (MDLAC) (Shi *et al.* 2000a), which is in line with the damage detection strategy employed in the sensor placement optimization, is used for damage localization. It is obtained by

$$\text{MDLAC}(\theta_k) = \frac{|\{\Delta\Phi\}^T \cdot \{\delta\Phi(\theta_k)\}|^2}{(\{\Delta\Phi\}^T \cdot \{\Delta\Phi\} \cdot \{\delta\Phi(\theta_k)\}^T \cdot \{\delta\Phi(\theta_k)\})} \quad (14)$$

where  $\Delta\Phi$  is the measured mode shape change before and after damage; and  $\delta\Phi(\theta_k)$  is the analytical mode shape change at the observed DOFs in the case that the structure has a reduction of stiffness properties in the  $k$ th member. MDLAC( $\theta_k$ ) performs as a correlation parameter between the true and pre-set damage cases. If damage occurs at the  $k$ th member, the value of MDLAC( $\theta_k$ ) will be close to 1. When MDLAC( $\theta_k$ ) is small, the two cases are uncorrelated, implying no damage at the  $k$ th member. This index is capable of preliminarily identifying damage location for further quantitative study.

The MDLAC index is applied to identify possible damage locations of the structure, respectively using noise-free and noise-corrupted mode shapes of the first 15 modes acquired from the 16-accelerometers configuration. A comparison of the damage localization results using the noise-free mode shapes from the optimally determined and existing in-service sensor configurations is shown in Figs. 4 to 7.

A higher MDLAC value in an element indicates that this element is more correlated with the true damage state. In this way, the potential damaged elements are identified and quantification of the damage extent can be subsequently performed for the damaged members. It is observed from Figs. 4 to 7 that the MDLAC obtained from the optimal sensor placement clearly indicates the

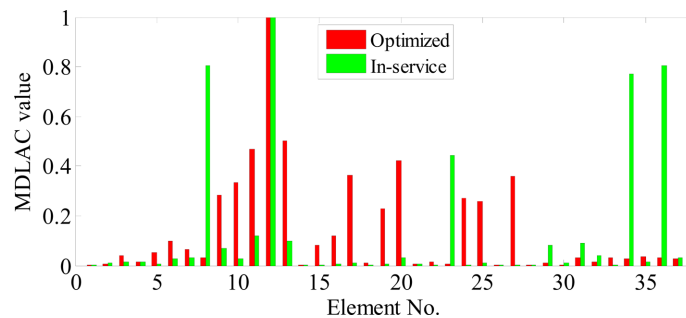


Fig. 4 Damage localization using noise-free measured data for damage case 1: damage in the 12th element

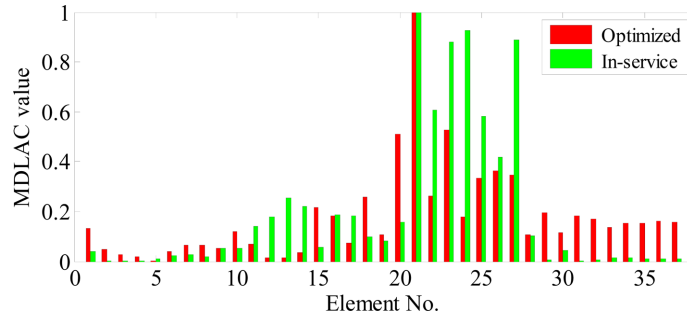


Fig. 5 Damage localization using noise-free measured data for damage case 2: damage in the 21st element

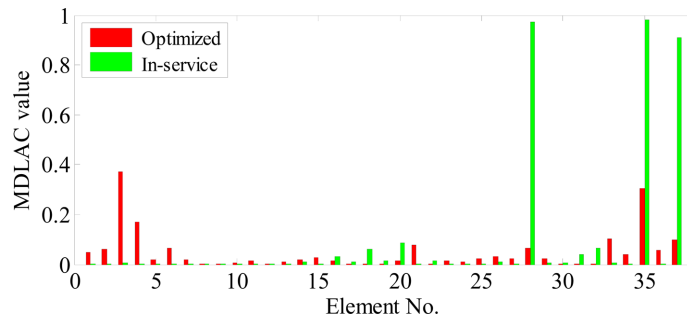


Fig. 6 Damage localization using noise-free measured data for damage case 3: damage in the 3rd and 35th elements

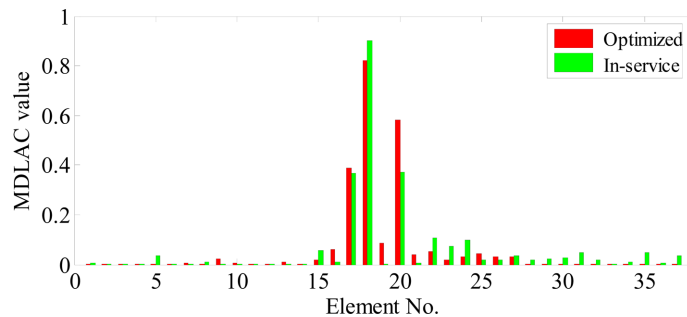


Fig. 7 Damage localization using noise-free measured data for damage case 4: damage in the 18th and 20th elements

damaged members in all single- and multi-damage cases, with its values for the damaged members being either close to 1 or distinctly higher than the values for other (undamaged) members. However, the MDLAC information obtained from the existing in-service sensor placement is insufficient to successfully locate the damage. In single-damage cases 1 and 2 with damage in the 12th element and the 21st element, respectively, the values of MDLAC obtained from the existing in-service sensor placement are less persuasive since there are several undamaged elements that have MDLAC values close to 1, although the MDLAC values indeed signal damage at the 12th and 21st elements, respectively. In multi-damage case 3 with damage at the 3rd and 35th elements, the values of MDLAC obtained from the existing in-service sensor placement wrongly indicate damage incurred simultaneously at the 28th, 35th and 37th elements. In multi-damage case 4 with damage at

the 18th and 20th elements, the values of MDLAC obtained from the existing in-service sensor placement signal false-positive damage at the 17th element with the value of MDLAC at this element being the same as that at the 20th element (a damaged element).

The damage localization results using the noise-corrupted (5% noise-to-signal ratio) mode shapes from the optimally determined and existing in-service sensor configurations are shown in Figs. 8 to 11.

Figs. 8 to 11 interpret the effect of noise on the damage localization results. Using the noise-corrupted measured data from optimal sensor placement, the MDLAC index gives an evident clue to identify the damaged elements. The MDLAC values of the damaged elements stand out among

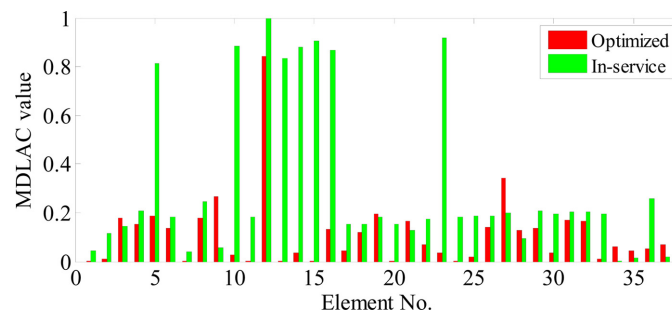


Fig. 8 Damage localization using noise-corrupted measured data for damage case 1: damage in the 12th element

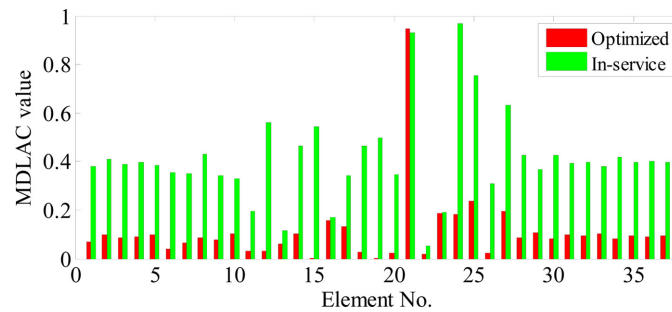


Fig. 9 Damage localization using noise-corrupted measured data for damage case 2: damage in the 21st element

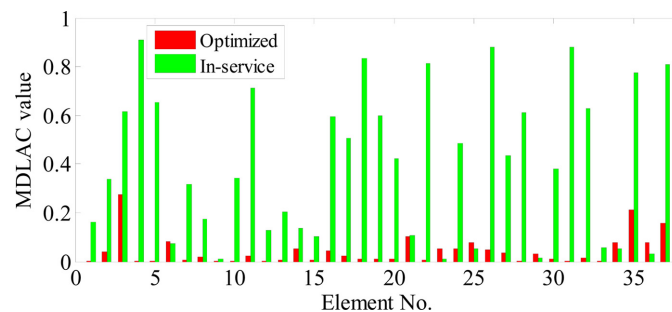


Fig. 10 Damage localization using noise-corrupted measured data for damage case 3: damage in the 3rd and 35th elements

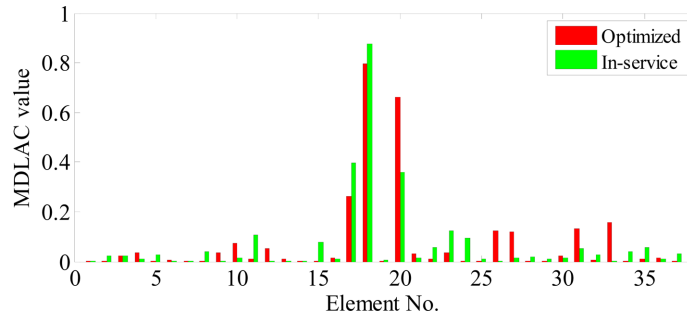


Fig. 11 Damage localization using noise-corrupted measured data for damage case 4: damage in the 18th and 20th elements

the values for all elements, although the distinctness is slightly compromised by noise. The worst result occurs in multi-damage case 3. The damage at the 35th element is not clearly indicated, since the MDLAC value of the 35th element is not much different than that of 37th element. More information or further identification is required to ensure the damage location. Looking at the localization results from the existing sensor placement, the MDLAC index could hardly indicate the damaged element(s), especially in multi-damage case 3. Preferable result occurs in multi-damage case 4, where the MDLAC index clearly indicates one damaged element (the 18th element); however, the MDLAC values of the 17th and 20th elements are the same. Further study into these two probable damage locations is required. By comparing the damage localization results from the optimized and existing in-service sensor configurations, it is concluded that the measured data from the optimized sensor configuration are more robust to noise than those from the existing sensor configuration.

#### 4.2 Optimal sensor placement for 20 accelerometers

##### 4.2.1 Simulation results

As part of the long-term SHM system for the Canton Tower, a total of 20 accelerometers have been permanently deployed on the main structure for real-time vibration monitoring (refer to Fig. 3). The proposed sensor placement optimization strategy is therefore performed again on the benchmark

Table 3 The optimally determined sensor placement when using 20 accelerometers

| Node number | Measurement direction | Node number | Measurement direction |
|-------------|-----------------------|-------------|-----------------------|
| 1           | X-axis                | 12          | X-axis                |
| 1           | Y-axis                | 12          | Y-axis                |
| 2           | X-axis                | 13          | X-axis                |
| 2           | Y-axis                | 13          | Y-axis                |
| 3           | X-axis                | 14          | X-axis                |
| 3           | Y-axis                | 14          | Y-axis                |
| 4           | X-axis                | 15          | X-axis                |
| 4           | Y-axis                | 15          | Y-axis                |
| 10          | X-axis                | 16          | X-axis                |
| 10          | Y-axis                | 16          | Y-axis                |

model, given that a total of 20 accelerometers are available. The optimally determined sensor placement in the case of 20 accelerometers is provided in Table 3.

#### 4.2.2 Verification

Damage detection in terms of the MDLAC index is then performed on the aforementioned four damage cases by use of both noise-free and noise-corrupted (5% noise-to-signal ratio) mode shape information obtained from the optimally determined sensor placement of 20 accelerometers. The damage localization results respectively using the noise-free and noise-corrupted measured mode shapes acquired from the 20 accelerometers are shown in Figs. 12 to 15.

It is found that both the noise-free and noise-corrupted mode shape data acquired from the placed sensors are able to reveal the locations of damage in the structure, and the MDLAC values of the

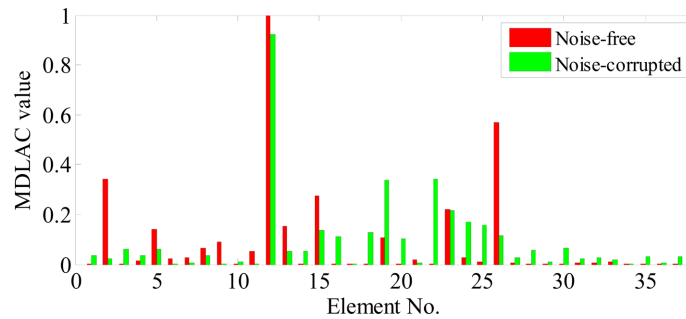


Fig. 12 Damage localization for damage case 1: damage in the 12th element

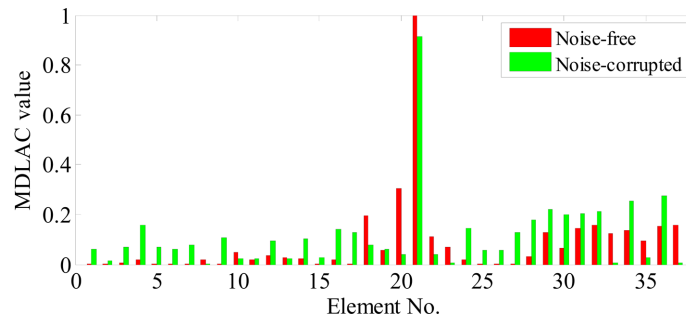


Fig. 13 Damage localization for damage case 2: damage in the 21st element

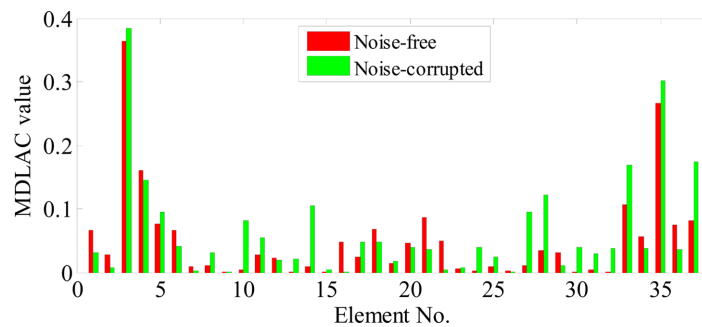


Fig. 14 Damage localization for damage case 3: damage in the 3rd and 35th elements

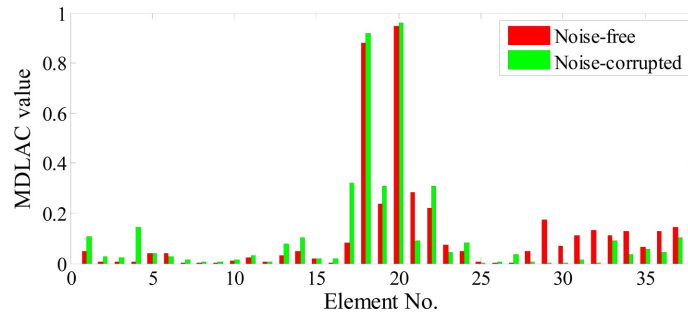


Fig. 15 Damage localization for damage case 4: damage in the 18th and 20th elements

damaged elements are generally much larger than those of the other (undamaged) elements. The noise-corrupted measured data from the placed sensor network remain informative enough for identifying the damage locations, and therefore show high robustness to noise. Moreover, by comparing the results from the two optimal sensor configurations with 16 and 20 accelerometers respectively, it is seen that the sensor network with four more sensors provides more distinct contrast for the MDLAC values between the damaged elements and the undamaged elements so that the damage locations can be identified more reliably.

## 5. Conclusions

This paper proposed a sensor placement strategy for the benchmark problem on optimal sensor placement with the target of damage detection. The damage pattern for the benchmark model and the information required for performing damage detection were specified. An information entropy index was introduced to measure the uncertainties over the damage detection process by use of the data obtained from the sensor configuration. Subsequently, a multi-objective optimization function was formulated from which the optimal solution was determined as the one that provided equally most informative data for all objectives and also provided most informative data for damage detection. To verify the efficiency of the optimally determined sensor placement configuration, damage localization using the mode shape information obtained from the placed sensors was performed on four damage cases, including both single- and multi-damage incurred in the benchmark model. The results show that in comparison with the existing in-service sensor configuration of the benchmark structure, the optimized sensor placement is capable of providing information more sensitive to structural damage and more robust to measurement noise. By comparing the damage localization results from the two optimal sensor configurations with 16 and 20 accelerometers respectively, it is found that the information obtained from the extra sensors enables more accurate and reliable damage identification.

## Acknowledgements

The work described in this paper was supported in part by grant from the Research Grants Council of the Hong Kong Special Administrative Region, China (Project No. PolyU 5263/08E) and

partially by a grant from the Hong Kong Polytechnic University through the Development of Niche Areas Programme (Project No. 1-BB68).

## References

- Beck, J.L. and Katafygiotis, L.S. (1998), "Updating models and their uncertainties I: Bayesian statistical framework", *J. Eng. Mech.- ASCE*, **124**(4), 455-461.
- Cobb, R.G. and Liebst, B.S. (1996), "Sensor location prioritization and structural damage localization using minimal sensor information", *AIAA J.*, **35**, 369-374.
- Doebbling, S.W. (1995), *Measurement of Structural Flexibility Matrices for Experiments with Incomplete Reciprocity*, Ph.D. Dissertation, Colorado University, USA.
- Fonseca, C.M. and Flemming, P.J. (1995), "An overview of evolutionary algorithms in multi-objective optimization", *Evolution. Comput.*, **13**, 1-16.
- Guo, H.Y., Zhang, L., Zhang, L.L. and Zhou, J.X. (2004), "Optimal placement of sensors for structural health monitoring using improved genetic algorithms", *Smart Mater. Struct.*, **13**(3), 528-534.
- Heo, G., Wang, M.L. and Satpathi, D. (1997), "Optimal transducer placement for health monitoring of long span bridge", *Soil Dyn. Earthq. Eng.*, **16**(7-8), 495-502.
- Imamovic, N. (1998), *Model validation of large finite element using test data*, Ph.D. Dissertation, Imperial College London, UK.
- Kammer, D.C. (1991), "Sensor placement for on orbit modal identification and correlation of large space structures", *J. Guid. Control Dynam.*, **14**(2), 251-259.
- Ni, Y.Q., Xia, Y., Liao, W.Y. and Ko, J.M. (2009), "Technology innovation in developing the structural health monitoring system for Guangzhou New TV Tower", *Struct. Health Monit.*, **16**(1), 73-98.
- Ni, Y.Q., Wong, K.Y. and Xia, Y. (2011), "Health checks through landmark bridges to sky-high structures", *Adv. Struct. Eng.*, **14**(1), 103-119.
- Ni, Y.Q., Xia, Y., Lin, W., Chen, W.H. and Ko, J.M. (2012), "SHM benchmark for high-rise structures: a reduced-order finite element model and field measurement data", *Smart Struct. Syst.*, in this issue.
- Meo, M. and Zuppano, G. (2005), "On the optimal sensor placement techniques for a bridge structure", *Eng. Struct.*, **27**(10), 1488-1497.
- Papadimitriou, C. (2004), "Optimal sensor placement methodology for parametric identification of structural systems", *J. Sound Vib.*, **278**(4-5), 923-947.
- Papadimitriou, C. (2005), "Pareto optimal sensor locations for structural identification", *Comput. Method. Appl. M.*, **194**(12-16), 1655-1673.
- Rao, A.R.M. and Anadakumar, G. (2007), "Optimal placement of sensors for structural system identification and health monitoring using a hybrid swarm intelligence technique", *Smart Mater. Struct.*, **16**(6), 2658-2672.
- Shi, Z.Y., Law, S.S. and Zhang, L.M. (2000a), "Damage localization by directly using incomplete mode shapes", *J. Eng. Mech. - ASCE*, **126**(6), 656-660.
- Shi, Z.Y., Law, S.S. and Zhang, L.M. (2000b), "Optimum sensor placement for structural damage detection", *J. Eng. Mech. - ASCE*, **126**(11), 1173-1179.
- Souza, D.K. and Epureanu, B.I. (2008), "Sensor placement for damage detection in nonlinear systems augmentations", *AIAA J.*, **46**(10), 2434-2442.
- Srinivas, N. and Deb, K. (1994), "Multi-objective optimization using non-dominated sorting in genetic algorithms", *Evolution. Comput.*, **2**(3), 221-248.
- Worden, K. and Burrows, A.P. (2001), "Optimal sensor placement for fault detection", *Eng. Struct.*, **23**(8), 885-901.
- Yuen, K.V., Katafygiotis, L.S., Papadimitriou, C. and Mickleborough, N.C. (2001), "Optimal sensor placement methodology for identification with unmeasured excitation", *J. Dyn. Syst. Measure. Control*, **123**(4), 677-686.